ISSN 0016-7029, Geochemistry International, 2006, Vol. 44, No. 7, pp. 690–703. © Pleiades Publishing, Inc., 2006.
Original Russian Text © A.Yu. Lein, Ya.A. Bogdanov, D.V. Grichuk, I.I. Rusanov, A.M. Sagalevich, 2006, published in Geokhimiya, 2006, No. 7, pp. 749–762.

Geochemistry of Hydrothermal Solutions from 9°50′ N at the East Pacific Rise (EPR) within Twelve Years after the Eruption of a Submarine Volcano

A. Yu. Lein[a], Ya. A. Bogdanov[a], D. V. Grichuk[b], I. I. Rusanov[c], and A. M. Sagalevich[a]

[a]*Shirshov Institute of Oceanology, Russian Academy of Sciences, Nakhimovskii pr. 36, Moscow, 117997 Russia*
e-mail: lein@geo.sio.rssi.ru

[b]*Geological Faculty, Moscow State University, Vorob'evy gory, Moscow, 119899 Russia*

[c]*Institute of Microbiology, Russian Academy of Sciences, pr. 60-letiya Oktyabrya 7, bldg. 2, Moscow, 117811 Russia*

Received October 28, 2004

Abstract—Hydrothermal solutions were examined in a circulation system that started to develop after the 1991 volcanic eruption in the axial EPR segment between 9°45′ N and 9°52′ N. Within the twelve years elapsed after the eruption, the diffusion outflow of hot fluid from fractures in basaltic lavas gave way to focused seeps of hot solutions through channels of hydrothermal sulfide edifices. The example of field Q demonstrates that the concentrations of H_2S decreased from 86 to 1 mM/kg from 1991 to 2003, and the Fe/H_2S ratio simultaneously increased by a factor of 1.7, a fact that can explain the disappearance of the microbial mats, which were widespread at the fields before 1991. The S isotopic composition of H_2S is independent of the H_2S concentration, a fact testifying to the rapid evolution of the hydrothermal system in the early years of its evolution. Carbon in CH_4 from the hot fluid sampled in 2003 is richer in the light ^{12}C isotope than carbon in the fluid from the hydrothermal field at 21° N in EPR, which suggests that methane comes to field Q from more than one source. The composition of particulate matter in the hydrothermal solutions indicates that it was contributed by biological material. Experimental solutions with labeled substrates ($t < 70$°C) show evidence of the active processes of methane oxidation and sulfate reduction. Our results indicate that, during the 12 years of the evolution of the hydrothermal system, the composition of its solutions evolved and approached the compositions of solutions in mature hydrothermal systems in EPR.

DOI: 10.1134/S0016702906070068

INTRODUCTION

New posteruptive hydrothermal fields were formed in 1991 in the axial zone of EPR, within a volcanic eruption field between 9°45′ N and 9°52′ N (Fig. 1) [1–6]. By the time when they were first examined by American researchers during DSRV *Alvin* dives, the age of the erupted basalts was less than two weeks.

The solutions were discharged directly via fractures in basaltic lava, because neither sulfide nor other hydrothermal edifices still had been formed. It was not until March of 1992 that the first sulfide towers up to 5 m high, from which sulfide-bearing solutions outpoured, were produced at the seafloor in the area. The most interesting results were the measurements of H_2S concentrations in the solution. In April of 1991 (so-called "Time Zero" [6]), the H_2S concentration in the fluids of some of the fields (A vent) reached 70 mM/kg, but it diminished to 11.3 mM/kg already in March of 1994.

Correspondingly, variations in the fluid composition resulted in changes in the biological community at the newly formed hydrothermal fields. Within one year after the eruption, close to 60% of the seafloor area of the hydrothermal filed was covered by pale microbial mats and rare isolated colonies of vestimentiferan *Tavnia jerichonana* [7]. Two years after the drastic decrease in the H_2S concentration in the solutions, the predominant organisms at the fields were vestimentiferan *Riftia pachiptila*. Three years afterward, the basaltic floor was inhabited by *Bathymodiolus thermophilus* mollusk. Crabs and polychaetes–serpulids appeared in the fields four years later, and mollusks colonized riftia tubes. Between the third and the fifth year after the eruption, the number of fauna species in the biological communities of the hydrothermal fields increased by two to three orders of magnitude. The researchers quoted above believed that mollusks would dominate in the communities of the newly formed hydrothermal fields during the following five–ten years.

A fairly interesting fact is that active hydrothermal fields with well-developed biological communities occurred at the area before the 1991 eruption, and these communities were burred beneath hot basaltic lavas [5, 7–9].

All transformations in the biological communities should have definitely occurred in response to changes in the geochemistry of the hydrothermal system.

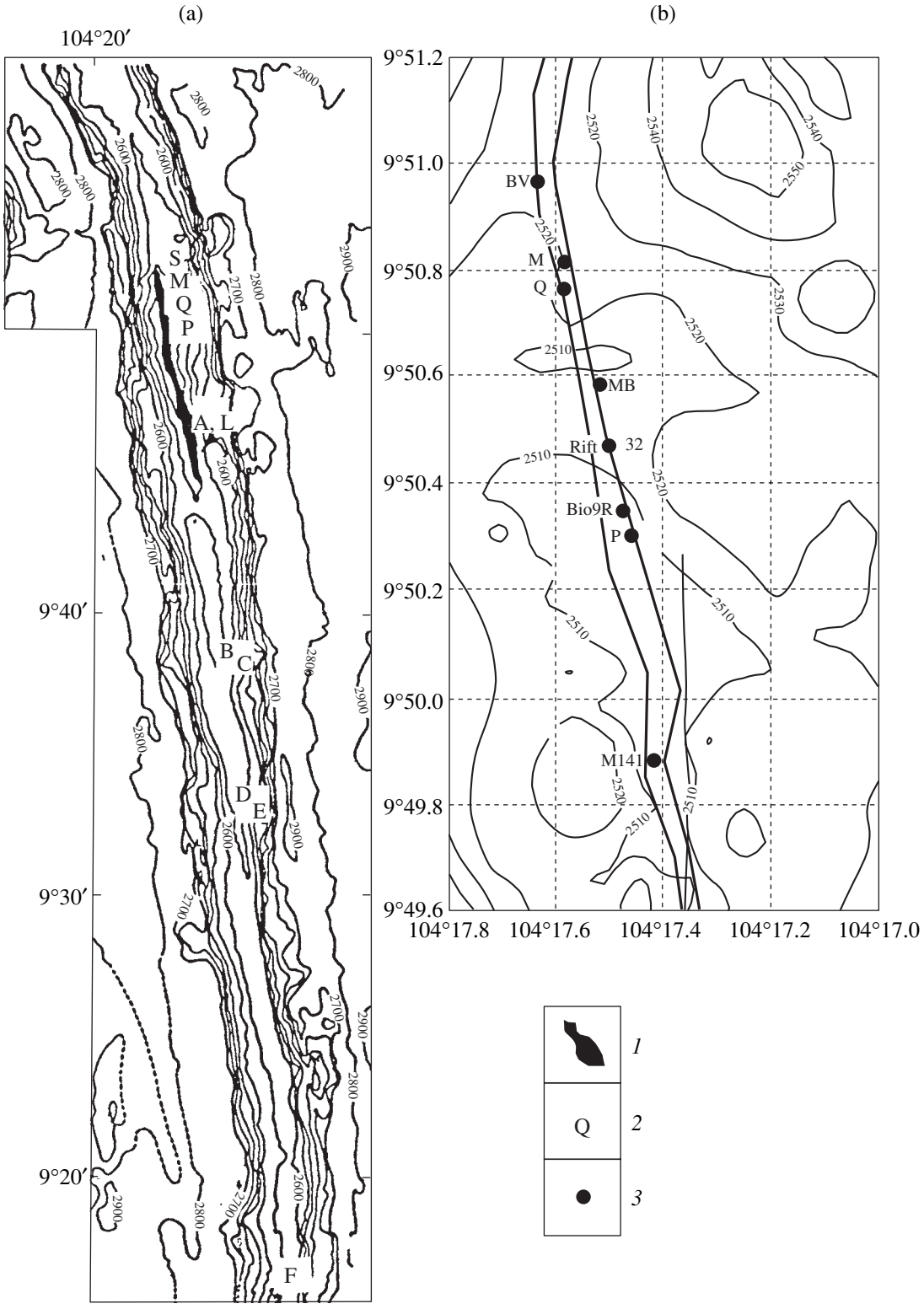

Fig. 1. Schematic map of (a) hydrothermal fields in the 9°10′–9°51′ N segment of EPR [1] and (b) sampling sites of hydrothermal solutions and deposits in the 9°50′–9°51′ N segment of EPR. (*1*) Zone where a submarine volcano erupted in 1991; (*2*) hydrothermal fields (indices) [1]; (*3*) sampling sites in 2003.

In September to early October of 2003, a research team from the Shirshov Institute of Oceanology and other institutes of the Russian Academy of Sciences got a chance to examine hydrothermal fields in the northern part of the 1991 volcanic eruption area (at 9°50′2 N–9°51′0 N at EPR) during a cruise of the R/V *Akademik Mstislav Keldych* with two submersibles (*Mir-1* and *Mir-2*) aboard (Fig. 1).

The task of this work was to trace the evolution of the fluid composition during the 12 years of the evolution of the circulation hydrothermal system at one of the segments of EPR.

GEOLOGICAL OVERVIEW

Our study area was located in the EPR segment between the Clipperton Fracture Zone at 10°10′ N in the north and the overlapping of two spreading centers at 9°03′ N in the south [10]. In this area, lithospheric plates spread with a velocity of 11 cm/year, i.e., the ridge is fast-spreading. Within this segment of the ridge, the depth and shape of its axial zone notably vary along the ridge axis. The deepest (2760 m) and relatively narrow (no wider than 2 km) axial zone with triangular (in cross section) topographic features is restricted to the southern most part of the segment.

The depth of the axial zone gradually decreases northward and reaches its minimum values of 2540–2520 m at 9°50′ N. Our studies were carried out in this part of the spreading ridge. The axial high is there up to 4 km wide, and it is trapezoidal or dome-shaped in cross section. The depth of the axial zone abruptly increases only in the vicinity of the fracture zone in the north of the area.

As has been demonstrated by geophysical evidence, the shallowest depths of the axial zone occur above the most elevated (closest to the seafloor surface) magmatic chamber (about 1.5 km from the seafloor surface), with the magmatic chamber somewhat deepening both south- and northward [10].

At the surface, the axial zone consists of relatively young volcanics, with the youngest of them spatially restricted to the shallowest depths between 9°37′ N and 9°51.5′ N. Judging from the amount of loose material on the surface, the character of the surface of the volcanics, and their first radiological dates, the age of these rocks ranges form 0 to 50 years. Many of the volcanics erupted in the spring of 1991 [8].

The central portion of the northern shallow-depth part of this segment includes a graben, which is often thought to be an elongated axial caldera but not a tectonic structure. The caldera may have been formed immediately after the cessation of volcanic activity, the partial emptying of the magmatic chamber, and the collapse of its roof. The width of this caldera was controlled by the depth of the roof of the crustal chamber. It is narrow (40–70 m) in the shallowest part of the zone, where the roof of the chamber occurs at the minimum depth. South of 9°44′, the caldera widens to 90–150 m, and the chamber roof deepens to 100–200 m. The depth of the axial part of the caldera is 5–10 m (sometimes more). The central part of the caldera is cut by a fracture from 1 to 5–8 m wide and up to 10 m (occasionally more) deep.

As was mentioned above, the study area coincides with the shallowest part of the axial zone of the ridge, its axial caldera and, within this caldera, with its axial fracture. Fractures intersecting the volcanic basement serve as pathways for the ascent of hydrothermal solution to the surface.

The ridge segment within our study area (approximately 1 km long) includes at least six active and a number of relict hydrothermal fields (Fig. 1). The more frequent occurrence of hydrothermal fields compared to their presence in the areas of hydrothermal processes within slow-spreading ridges is one of the distinctive features of the active rifts of fast-spreading ridges.

The fields were determined to host two types of hydrothermal activity: low-temperature (with widespread diffusion seeps) and high-temperature (with sulfide edifices).

Anomalous hydrothermal fauna colonies were found in the low-temperature hydrothermal fields. These organisms inhabit the surface of volcanic rocks practically devoid of hydrothermal mineralization. The warm solutions collected at the hydrothermal field are represented by samples 4622-M1-Tb, 4623-M2-Tb, and 4623-M2-BN (Table 1).

The high-temperature hydrothermal mineralization within the study area includes two types. Type I comprises of plates up to 10–15 cm thick that cover the basement basalts. Most of them are covered by films of iron oxides and are relicts. They are layered, with the lower parts of the plates (adjacent to the basalt surface) consisting of the highest temperature, predominantly copper mineralization. The plates are overlain by a layer of anhydrite and, often, layers of lower temperature hydrothermal sulfides. In places, the hydrothermal plates are topped by small (no higher than 0.5 m) relict hydrothermal pipes.

It is important to mention that the lower parts of the plates may contain relict channels that served as pathways for high-temperature mineralized hydrothermal solutions discharged from fractures in the basalts [8].

The other type of high-temperature hydrothermal features (both active and relict) comprises conical columnar hydrothermal edifices.

Field BV (Fig. 1), in which low-temperature diffuse seeps are widespread, includes a single active high-temperature hydrothermal edifice. This is a pillar about 3 m in diameter near its bottom and approximately 6 m high, which slightly tapers upward. The pillar consists of "coalescent" hydrothermal pipes, with some of them protruding as spires from the upper part of the pillar. Some of these spires are still active. They may discharge transparent waters or solutions with gray

Table 1. Brief characterization of hydrothermal solutions

No.	Sampling date	Sample	Field index	Brief characterization of samples	pH	DOC, mg/l
1	Sept. 21, 2003	4654-M1-Tb	Q	Bottom water	7.60	–
2	Sept. 6, 2003	4626-M2-Tb	Q	Black smoker	4.90	–
3	Sept. 8, 2003	4632-M2-Tb	Q	″	5.16	4.09
4	Sept. 15, 2003	4637-M1-Tb	BV	Black smoker (edifice wall)	5.68	4.37
5	Sept. 16, 2003	4642-M2-Tb	BV	Black smoker	5.25	4.22
6	Sept. 21, 2003	4655-M2-Tb	Q	″	5.60	–
7	Sept. 30, 2003	4666-M1-Tb	Q	″	5.40	–
8	Sept. 30, 2003	4667-M2-Tb	Q	″	6.30	–
9	Oct. 1, 2003	4668-M1-Tb	Q	″	3.80	2.62
10	Oct. 2, 2003	4671-M2-Tb	Q	″	5.22	–
11	Sept. 5, 2003	4622-M1-Tb	MB	Warm spring (moire)	7.58	6.56
12	Sept. 5, 2003	4623-M2-Tb	MB	Powerful warm spring (moire)	5.90	–
13	Sept. 5, 2003	4623-M2-BN	MB	Moire	6.90	–
14	Sept. 8, 2003	4631-M1-Tb	Q	White smoker	6.10	3.81
15	Sept. 6, 2003	4626-M2-BN	Q	Smoke zone of a black smoker	7.00	
16	Sept. 8, 2003	4632-M2-BN	Q	″	6.90	3.19
17	Sept. 21, 2003	4655-M2-BN	Q	″	7.48	–
18	Sept. 28, 2003	4665-M2-BN	Q	″	7.04	–

Note: The solutions were sampled at a depth of 2520 m; coordinates of fields: Q – 9°50.7′ N, BV – 9°50.9′ N, MB – 9°50.6′ N; DOC means dissolved organic carbon; analyses were conducted at VNIRO; here and below, dashes mean the absence of data.

"smokes" (samples 4637-M1-Tb and 4642-M2-Tb, Table 1). Low-temperature diffusion outflows were detected at the walls of the pillar. The three sides of this pillar rest on a basaltic basement, and only one of its sides towers above the basement of relict plates.

In field M (Fig. 1), three conical (spire-shaped) sulfide edifices (elongated meridionally) rest on a single basement. It should be emphasized that this basement consists of sulfide plates and is not brecciated (as is the case with most hydrothermal fields). These edifices are 3–6 m high and reach 2–3 m in diameter near their bottoms. The edifices are spaced 2–3 m apart. The nearby basement contains a volcanic (basaltic) pillar with closely spaced horizontal ribbing, which is typical of the area. The sulfide spire-shaped edifices consist of merged hydrothermal pipes, some of which protrude from the slopes of the edifice in the form of spire-shaped pipes.

Active pipes at the tops of the edifices are black and gray smokers, whose apexes are sometimes inhabited by vestimentiferan thickets, whereas the remaining parts of the sulfide edifices are devoid of biota. The sulfides composing the edifices are pale brown at the surface owing to the presence of iron oxy-hydroxides.

Two conical edifices spaced 6–8 m apart were discovered at field Q (Fig. 1). One of them is 7 and the other is 12 m high, and they are 3 and 5 m, respectively, in diameter near their bottoms. Both edifices are merged hydrothermal pipes, some of which are topped with high spires. The higher edifice is a black smoker, whose solution was examined in much detail (sample 4621-M2-Tb, Table 1). The upper part of the lower edifice is characterized by moire outflows of low-temperature hydrothermal solutions (sample 4631-M1-Tb, Table 1). Diffuse hydrothermal seeps were also detected at the walls near the bottoms of the hydrothermal edifices. We also examined samples of solutions from the black-smoke zone of smoker Q. Both edifices are located directly on the surface of the volcanic basement. Relatively short hydrothermal plates were found near one of the edifices.

A number of conical edifices up to 8 m high were detected at hydrothermal field P (Fig. 1). Some of these edifices have seeps of high-temperature hydrothermal solutions with black smokes at their tops and in the bottom parts, as well as accumulations of sulfide fragments (that fell from the walls) near the bottoms. The edifices rest on a basement of relict hydrothermal plates. The area with the plates also includes relict pipes 1.5 m high, whose upper parts have diffusers.

Small hydrothermal sulfide edifices were detected at the tops of the volcanic pillars. They are fed from channels in the central parts of the pillars.

The plates and conical edifices mark the initial evolution of the hydrothermal circulation system and the early evolutionary stages of the orebodies. Immediately

Table 2. Analytical techniques used in this study [11, 12, appended]

Element or compound	Method	Accuracy
pH (25°C, 1 atm)	Potentiometry	±0.01
Alk_{tot}	Potentiometric titration	±0.5%
H_2S	Iodometric titration	±5%
CH_4	Gas chromatography	±5%
H_2	"	±5%
$\delta\,^{34}S$ (CDT)	Mass-spectrometry	±0.2‰
$\delta\,^{13}C$ (PDB)	"	±0.2‰
Cl	$AgNO_3$ titration	±1%
Mg	Trilonometry	±0.5%
Ca	"	±0.5%
Fe	Flame atomic absorption	±1%
Mn	"	±1%
Zn	"	±1%
Cu	"	±1%
Co	Electrothermal atomic absorption	±20%
Ni	"	±20%
Ag	"	±20%
$^{14}CO_2$ assimilation	Radioisotopic with labeled substrates	±0.00*n*%
$^{14}CH_4$ synthesis	"	±0.00*n*%
$^{14}CH_4$ oxidation	"	±0.00*n*%
$^{35}SO_4$ reduction	"	±0.00*n*%

after volcanic activity in the spring of 1991, the major outflow mode of the hydrothermal solution (including that of the low-temperature hydrothermal solutions) was diffusion, as was observed during DSRV dives shortly after volcanism. The areas with diffusion outflow drastically diminished with time. This process was associated with the origin of seeps with a strong focused discharge of hydrothermal solutions and with growing edifices in the form of pillars and spires composed of lower temperature sulfide mineralization.

These edifices sometimes occur on older hydrothermal plates, which serve as the basements for the edifices. However, some edifices rise directly from the basaltic basement. It is important to mention that these two types of the hydrothermal edifices are not coeval, a fact that has never been noted before at other fields in oceanic rifts.

It is also pertinent to mention another feature detected at the fields: most researchers explain the cyclicity in the hydrothermal activity within rifts by the alternation of volcanic and tectonic cycles in the evolution of spreading ridges. It is, however, senseless to refer to tectonic cycles in reference to our study. The alternation of cycles of volcanic and hydrothermal activity is controlled solely by variations in the volcanic activity with time. Upon the cessation of a volcanic cycle and the partial emptying of the crustal magmatic chamber, its roof collapsed, and, consequently, pathways were formed for the ascent of hydrothermal solutions. The duration of the hydrothermal cycles was determined by the velocity of the filling of the partly emptied magmatic chamber with basaltic melt.

MATERIALS AND METHODS

From September 6 to October 2, 2003, nine solution samples were collected at black smokes within fields BV and Q, four warm solutions were sampled at fields MB and Q, and four samples of bottom waters were taken from the black-smoke zone (Table 1).

The solutions were sampled during the dives of *Mir-1* and *Mir-2* submersibles, using remote Ti bathometers (Tb) 500 and 750 ml in volume (modified design of the Institute of Experimental Mineralogy, Russian Academy of Sciences, in Chernogolovka, Moscow oblast).

Bottom waters from the black-smoke zone and partly from the moire were sampled with 30-l Niskin bottles (NB) that were fixed on the sides of the submersibles.

The analytical techniques used in this research are listed in Table 2. Immediately after the lifting of the submersibles, water aliquots from the bathometers were taken to measure pH, Alk, and H_2S. The results of

these measurements allowed us to roughly evaluate the dilution of the hydrothermal fluid by seawater.

The next stage of our work with the bathometers involved the sampling of the solution for determining their methane concentrations and for collecting the gas phase in special vessels, which were blown with argon and contained a salt solution, to examine the isotopic compositions of the gases in the laboratory. Some of the samples were utilized for microbiological studies with the aim of determining the rates of major microbial processes of chemosynthesis, methanotrophy, methanogenesis, and sulfate reduction in experiments with the addition of substrates doped with ^{14}C and ^{35}S [11, 12].

The major-salt composition of the solutions and the concentrations of dissolved C_{org} were determined in frozen samples of the solutions acidified to pH 2.

We managed to collect the particulate material of some solution samples to determine the composition of this material and the isotopic composition of its organic carbon.

The recalculated end-member composition of the least diluted sample of the hot fluid from sulfide edifice Q (sample 4668-M1-Tb) was compared with the chemical composition of solutions from field Q and other fields that were sampled after the 1991 eruption.

RESULTS AND DISCUSSION

Chemical composition of the solutions of black smokers. The samples of the solutions from black smokers with pH from 5.68 to 4.9 had Cl, Mg, and Ca concentrations close to those in the ambient seawater, whereas the sample with pH 3.8 was richer in Cl and Ca and poorer in Mg than the seawater (Table 3). The concentrations of metals in all the samples from black smokers were much higher (by three orders of magnitude) than in the bottom water, particularly in the least diluted sample 4668-M1-Tb from field Q (Table 3). Most of the samples contained H_2S and CH_4, with the maximum concentrations of gases found in sample 4668-M1-Tb from field Q.

In order to compare the results of chemical analyses of the solution collected in 2003 with earlier measurements at filed Q and other fields, the composition of sample 4668-M1-Tb was recalculated with respect to the zero Mg concentration (end member) (Table 3). The recalculated data indicate that the solution from field Q contains one order of magnitude more Cl and 1.5 times more Fe and Mn than the analogous concentrations in the solution collected in 1991, whereas the H_2S concentration simultaneously decreased from a maximum value of 33.4 to 4.02 mM/kg (Tables 3, 4).

The low mineralization of the solutions in the 1991 samples suggests that they were contributed by great amounts of condensed vapor. The fact that the Cl concentration approached the values characteristic of seawater means a diminish in the role of subsurface boiling (up to its complete disappearance) during the 12 years when the observations were conducted. The positive correlation between the concentrations of metals and Cl and the negative correlation between H_2S and Cl was documented previously at some other hydrothermal systems [18]. This phenomenon can be explained by the fact that volatiles (including H_2S) are redistributed into the gas phase during subsurface boiling, whereas Cl and metals enriched the boiling solution. The data obtained from seeps at field Q are consistent with this hypothesis.

Proportions of the H_2S and Cl concentrations analogous to those in the solution from field Q were detected in the solutions from nearby hydrothermal fields. Anomalously high H_2S concentrations (up to 86 mM/kg) in solutions at their low Cl contents were detected in 1991 at seven of the hydrothermal fields (Fig. 2). Some of the solutions also showed analogous relations in 1992. Starting in 1994, the H_2S concentrations in the solutions did not exceed 10–11 mM/kg and occasionally decreased to 1–2 mM/kg at Cl concentrations ranging from 350 to 860 mM/kg. The H_2S and Cl concentrations measured in 2003 corresponded to the ranges of analogous values from the thoroughly examined "mature" EPR segment at 21° N (Fig. 2). This fact suggests that the hydrothermal system at 9°50′7 N evolved over the past twelve years from the state of an unstably developing system with extensive boiling to a typical stable circulation hydrothermal system in a fast-spreading ridge.

Isotopic composition of H_2S in the solutions of black smokers. The values of $\delta^{34}S$–H_2S in the hot fluid in April of 1991 were 5.5‰ at field Q and reached 7.8‰ in adjacent fields (Table 3, Figs. 3, 4). The systematic changes in the isotopic composition of the solution from field Q were detected on March 22, 1994 ($\delta^{34}S$ = 5.8‰) and March 30, 1994 ($\delta^{34}S$ = 3.5‰) [13], i.e., within one week, demonstrate that the hydrothermal system continued to evolve.

The $\delta^{34}S$ values in the hot fluid from field Q were 3.3‰ (average of three measurements) during the 25 days when our expedition worked and approached the field of values of $\delta^{34}S$–H_2S for the solution from 21° N (Fig. 3, Table 3).

The early evolution of the hydrothermal system was characterized by a generally weak correlation between the $\delta^{34}S$ of H_2S and the concentration and time that elapsed from the last eruption. It is reasonable to expect that "maturing" of the systems should be associated with reaching less variable values of $\delta^{34}S$–H_2S in the solution and lower ^{34}S concentration in it than the analogous concentration during the early evolutionary stages of the hydrothermal activity.

Sulfur isotopic composition of sulfide ore minerals. Sulfide minerals from active pipes and diffusers at fields Q and BV are isotopically heavier than sulfide

Table 3. Chemical composition of the hot fluids (end members) from hydrothermal fields at 9°50.7′ N (field Q), 9°17′ N (field F), and 21° N, EPR

Component	Unit of measure	Q_{1991} Aprl. 19, 1991 "time zero"	Q_{1994} March 22, 1994	Q_{1994} March 30, 1994	Q_{1995} Nov. 18, 1995
t	°C	371	293	297	310
pH		2.8	–	–	–
Alk	g-equiv./l	–1.05	–	–	–
Cl	mM/kg	71.4	490	480	571
Mg	mM/kg	0.0	–	–	–
Ca	mM/kg	0.805	–	–	–
Fe	mM/kg	1470.0	–	–	–
Mn	mM/kg	187.0	–	–	–
Zn	mM/kg	–	–	–	–
Cu	mM/kg	–	–	–	–
Ag	mM/kg	–	–	–	–
H_2S	mM/kg	33.4 (max)	3.7	9.9	–
CH_4	mM/kg	115 and 74*	–	–	–
Fe/Cl		0.0206	–	–	–
Fe/Mn		7.8	–	–	–
Mn/Cl		0.0026	–	–	–
H_2S/Cl		0.44	–	–	–
Fe/H_2S		0.36	–	–	–
$\delta\,^{34}S$–H_2S	‰	5.5	5.8	3.5	–
$\delta\,^{13}C$–CH_4	‰	–	–	–	–
DOC	mg/l	–	–	–	–
References		[6, 13, 14]	[1]	[1]	[1]

Component	Q_{2003} Sept. 1, 2003 4668-M1-Tb	F_1 Aprl. 16, 1991	F_2 March 15, 1994	21° N	Seawater
t	–	388	351	273–355	2
pH	3/1	2.8	2.6	3.3–3.8	7. 8
Alk	–1.29	–1.4	–1.8	–0.19 … –0.50	2.3
Cl	580.4	46.5	846.0	489–579	541
Mg	0.0	0.0	0.0	0.0	52.72
Ca	51.15	1.83	45.6	11.7–20.8	10.2
Fe	2452.0	1490	12100	750–2429	0.0045
Mn	321.4	174	3280	699–1002	0.0013
Zn	30.7	–	–	40–106	0.028
Cu	11.8	–	–	<0.02–44	0.0033
Ag	0.0086	–	–	<1–38	0.00002
H_2S	4.0	48.8	8.71	6.6–8.4	0.0
CH_4	6.0	–	–	1.9–55.0	–
Fe/Cl	0.0042	0.032	0.0143	0.0034	–
Fe/Mn	7.7	8.56	3.69	1.73	–
Mn/Cl	0.0055	0.037	0.0039	0.0020	–
H_2S/Cl	0.007	0.882	0.0103	0.0149	–
Fe/H_2S	0.61	0.0363	1.39	0.23	–
$\delta^{34}S$–H_2S	3.3 (average of 3)	6.4	6.7	1.3–3.4	–
$\delta^{13}C$–CH_4	–22.0 (average of 3)	–	–	–15.0 … –17.4	–
DOC	2.62	–	–	–	–
References	This paper	[4, 12]	[4, 12]	[15, 16]	[17]

* A-vent, 1991 and 1992 [4].

Table 4. Isotopic composition of S and C_{org} of sulfide ore from hydrothermal fields at 9°50.7′–9°50.9′ N

No.	Sample	Description	$\delta^{34}S$, ‰	$\delta^{13}C$–C_{org}, ‰
	4622-4 (BV)	Active pipe		
1		top	3.8	–29.0
2		middle part	3.8	–29.3
3		bottom	4.1	–29.1
4	4668-1 (Q)	Active pipe	3.8	–27.1
5	4625-3 (P)	Diffuser	4.0	–29.0
6	4658-2 (P)	Diffuser	3.9	–28.1
7	4626-2 (Q)	Relict pipe	2.6	–27.6
8	4637-3 (M)	Relict pipe	2.2	–32.6
9	4658-4 (P)	Relict pipe	2.5	–31.6
10	4658-6 (Q)	Plate	2.7	–22.4
11	4658-7 (BV)	Plate	2.2	–24.8
12	4658-11 (BV)	Plate	2.8	–25.0
	Average		3.1	–27.2
	9°–10° N*	Sulfide minerals	from 0 to –4	–

* Data from [1].

minerals from the earlier hydrothermal plates and relict pipes (Table 4).

Available literature data on the sulfur isotopic composition of sulfide minerals at 9°–10° N within an EPR cluster in the range of $\delta^{34}S$ = 0–4‰ [1], i.e., these minerals are isotopically lighter than H_2S in the hydrothermal solutions. The relations between the isotopically lighter sulfide minerals and H_2S enriched in the ^{34}S isotope were documented at 24 of the 27 sampled hydrothermal fields quoted in [18].

Methane concentrations and isotopic composition. The maximum methane concentration in the hot solution was 6.04 μM/kg (Table 3) and lies within a range of methane concentrations in the solution from 21° N at EPR. For comparison, it seems to be pertinent to quote the methane concentrations in the fluid from the A vent sampled in 1991 (0.015 mM) and 1992 (0.074 mM) [14]. Hence, the methane concentrations in the fluids decreased compared with those during the early evolution of the system.

The values of $\delta^{13}C$ of the methane are equal to –22.0‰ (compare with $\delta^{13}C$–CH_4 of fluid from 21° N: from –15.0 to –17.4‰; Table 3) and approach the isotopically lightest $\delta^{13}C$ values typical of methane from solutions at southern EPR segments: Nadir [$\delta^{13}C$ = –23.9‰] and Akorta [$\delta^{13}C$ = –22.0‰] [15, 19–21].

Concentrations of C_{org} dissolved in fluids (DOC). The lowest DOC concentration (2.62 mg C/l) was detected in the hot weakly diluted solution of sample 4668-M1-Tb (Table 1). In all other samples, the DOC concentrations varied from 3.19 to 4.37 mg C/l. The maximum DOC content was found in the solution of a powerful warm spring (sample 4623-M2-Tb, Table 1) surrounded by a densely populated biological community. The increase in the DOC concentration in the hot solution is most likely explained by the amount of the ambient seawater captured during the sampling. The DOC concentration in the warm spring was controlled, first of all, by the synthesis of C_{org} in the solution itself.

Concentrations of C_{org} in the particulate matter from the solutions and $\delta^{13}C$–C_{org} values of this particulate matter. The maximum amounts of particulate matter were detected in the water sample from a powerful warm spring (sample 4623-M2-Tb) and in the sample of the least diluted solution (sample 4668-M1-Tb) (Table 2).

Bottom waters in the black-smoke zone contained two orders of magnitude less particulate matter, and the transparent bottom waters sampled with Niskin bottles at the Rozette complex at a depth of 170 m and up the profile contained no more than 1.3 mg/l of particulate matter (Table 5).

The values of $\delta^{13}C$–C_{org} in the particulate matter from bottom water samples lie within the range from –11.5 to –23.1‰ (Table 5). Hence, the samples with isotopically heavy C_{org} are dominated by symbiotrophic microorganisms and fragments of vestimentiferan tissues ($\delta^{13}C$ from –9 to –11.5‰), whereas other samples contain mostly plankton-related organic matter (OM with $\delta^{13}C$ = –23‰), free-living microorganisms ($\delta^{13}C$ ~ –25‰), and OM of a mixed origin. The isotopic composition of C_{org} in the particulate matter from the solution of the powerful warm spring corresponded to

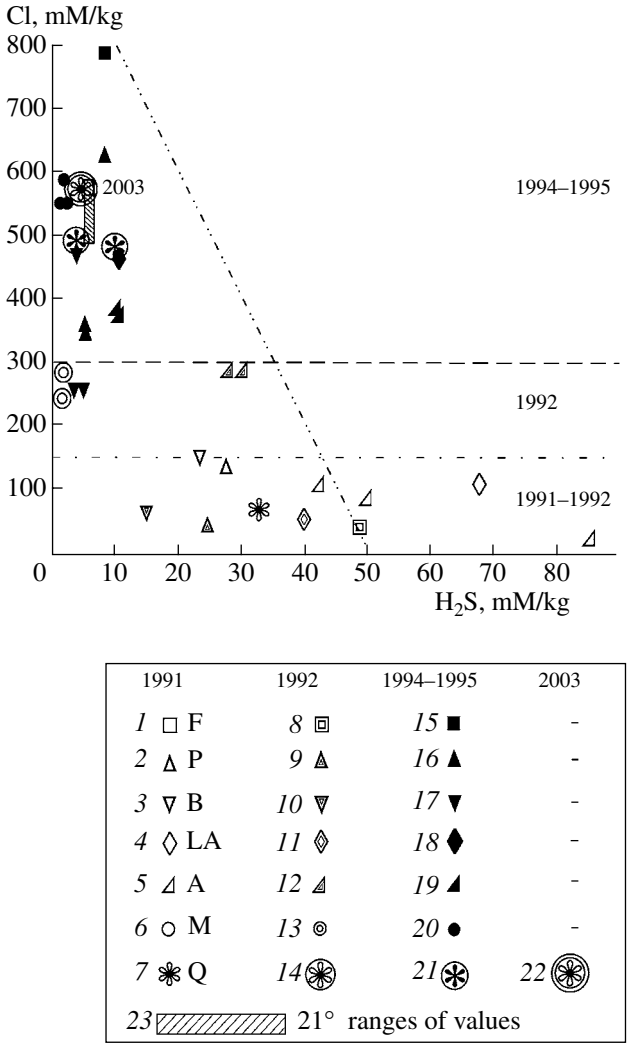

Fig. 2. Variations in the H_2S and Cl concentrations in fluids from hydrothermal fields within EPR from 1991–2003 in the vicinity of the submarine volcano eruption [modified after 1]. (*1–22*) Solution samples from hydrothermal fields collected in 1991 (open symbols), 1992 (half-shaded symbols), 1994–1995 (filled symbols), and 2003 (asterisk); 23°–21° N at EPR (ranges of values). Samples from fields: F—*1, 8, 15*; P—*2, 9, 16*; B—*3, 10, 17*; LA—*4, 11, 18*; A—*5, 12, 19*; M—*6, 13, 20*; Q—*7, 14, 21, 22*.

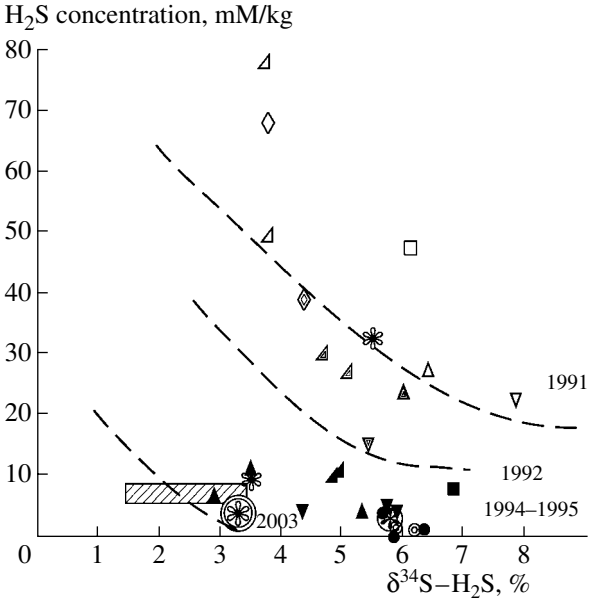

Fig. 3. Correlation between the $\delta^{34}S–H_2S$ and H_2S concentrations in fluids from hydrothermal fields sampled at different times [modified after 1]. See Fig. 2 for symbol explanations.

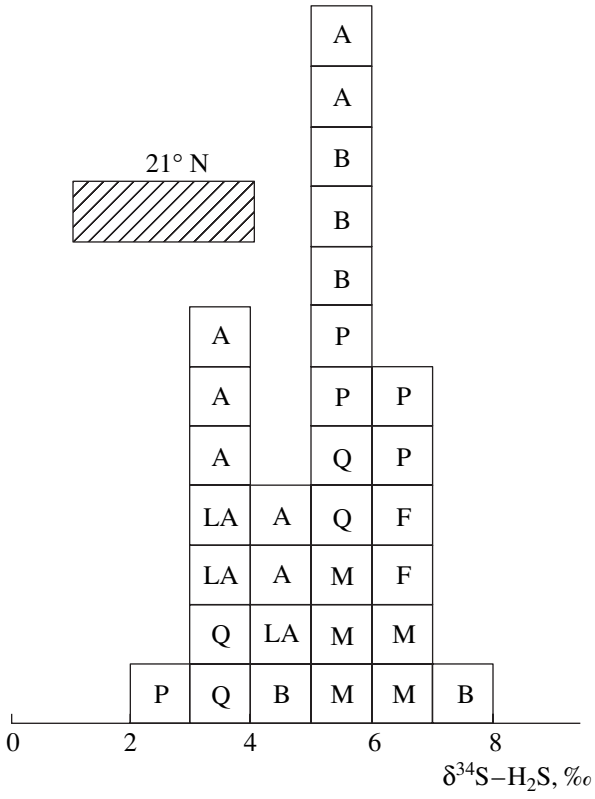

Fig. 4. Histogram of $\delta^{34}S–H_2S$ values in fluids from hydrothermal fields [modified after 1]. The shaded field corresponds to the $\delta^{34}S–H_2S$ values of fluids from "mature" hydrothermal fields at 21° N within EPR. Letters—indices of hydrothermal fields at 9°–10° N in EPR.

–25.4‰. As was mentioned above, the area around this spring is inhabited by all species of the local hydrothermal community, from microbes and vestimentiferans to mollusks, crabs, and polychaetes, with the $\delta^{13}C$ of C_{org} in the biomass of members of this community broadly varying from –9 to –35‰ [22].

Isotopically light carbon was identified in the biomass of the tissues of mollusks (*Bathymodiolus thermophilus*), which are widespread at 9° N (Table 6).

The first data were obtained on the isotopic composition of C_{org} in the particulate mater from the hot fluids. The values of $\delta^{13}C–C_{org}$ of particulate matter from the

Table 5. Content of particulate matter in water samples from hydrothermal fields at 9°50.7′–9°50.9′ N and $\delta^{13}C$–C_{org} of particulate matter from solutions and bottom waters

No.	Sample	Content of particulate matter, mg/l	Particulate matter weight, GF/F, mg	C_{org} concentration in particulate matter, %	$\delta^{13}C_{org}$ of particulate matter, ‰
		Hot fluids of black smokers			
1	4626-M2-Tb	250.0	32.5	0.024	–40.7
2	4632-M2-Tb	108.6	38.0	0.075	–43.6
3	4637-M2-Tb	204.0	30.6	–	–42.7
4	4642-M2-Tb	309.0	30.9	0.05	–40.3
5	4655-M2-Tb	97.5	39.0	0.013	–48.0
6	4668-M1-Tb	632.0	31.6	0.047	–38.0
7	4671-M2-Tb	301.0	30.1	0.045	–36.7
		Warm solutions from moires			
8	4622-M1-Tb	115.7	34.7	–	–41.3
9	4623-M2-Tb	707.5	56.6	–	–25.4
10	4631-M1-Tb	159.1	36.6	–	–46.5
		Bottom water in black-smoker zone			
11	4626-M2-BN	6.0	30.0	–	–11.6
12	4332-M2-BN	6.7	30.7	–	–21.8
13	4655-M2-BN	5.7	28.4	–	–13.8
14	4665-M2-BN	7.4	29.6	–	–23.1
		Bottom water at depths of 170–720 m above field Q			
15–17	4635-ROZ (three samples)	1.14–1.31	–	–	–
18–20	4636-ROZ (three samples)	1.17–1.18	–	–	–
		Bottom water outside the field at a depth of 2617 m			
21	4636-ROZ	1.25	–	–	–

Table 6. Carbon isotopic composition of mollusk tissues* at hydrothermal fields at 9°50.7′ N

No.	Site	Mollusk	Tissues	$\delta^{13}C$–C_{org}, ‰
1	4623	*Bathymodiolus thermophilus* (large)	Gills	–35.03
2	″	″	Foot	–32.74
3	″	″	Mantle	–33.66
4	″	″	Other tissues	–33.98
5	″	*Bathymodiolus thermophilus* (small)	Gills	–34.62
6	″	″	Foot	–33.12
7	″	″	Mantle	–33.38
8	″	″	Other tissues	–33.52
9	4668	*Bathymodiolus thermophilus* (medium-sized)	Gills	–32.76
10	″	″	Foot	–32.28

* S.V. Galkin's collection.

Table 7. Rates of microbiological processes in hot and warm solutions at hydrothermal fields at 9°50.7′–9°50.9′ N

No.	Sample	Description	pH of solution sample	*t*, °C of incubation	Assimilation of $^{14}CO_2$, ng C/l day	CH_4 oxidation, nl C/l day	Sulfate reduction, nl S/l day
1	4626-M2-Tb	Black smoker (field Q)	4.90	70	20	389.79	–
2	4632-M2-Tb	″	5.16	70	2870	909.23	–
3	4637-M1-Tb	Black smoker (field BV)	5.68	25	2070	135.53	1940
4	4646M2-Tb	″	5.25	70	1930	419.23	0
5	4655-M2-Tb	Black smoker (field Q)	5.60	70	3910	229.91	3444
6	4668-M1-Tb	″	3.80	70	100	577.31	2700
7	4671-M2-Tb	″	5.22	70	–	247.87	–
8	4622-M1-Tb	Warm spring (field MB)	7.58	5	760	2.22	–
				25	1970	2.12	–
				70	90	2.81	–
9	4623-M2-Tb	″	5.90	5	760	495.25	–
				25	9290	296.19	–
				70	980	366.17	–
10	4632-M2-BN	Smokes of a black smoker (field Q)	6.90	5	120	9.41	–
				25	2660	19.15	–

hot fluids varies from –36.7 to –48.0‰ (Table 5). It is quite difficult to explain these data. There can be more than one mechanism able to produce such isotopically light C_{org} in hot solutions, but all of these mechanisms are hypothetical.

First, the high-temperature abiogenic synthesis of carbon-bearing compounds is coupled with kinetic isotopic effects that can result in a notable depletion of the ^{13}C isotope in these carbon-bearing compounds ($\delta^{13}C$ from –25 to –50‰) [23, 24].

Another explanation relies on the assumption of the involvement of the pyrolitically modified OM of the biological community that functioned before April of 1991 at 9°–10° N and was then buried alive beneath newly erupted basalts of EPR [5, 7].

Finally, we cannot rule out the occurrence of a near-surface microbial biosphere with very low reaction rates, which led to significant fractionation of carbon isotopes.

Rates of the main microbial processes in solutions. It was determined in experiments with labeled compounds in samples of hydrothermal solutions that the most active microbial chemosynthesis (dark bacterial assimilation of $^{14}CO_2$) takes place in a solution of a powerful warm spring (sample 4623-M2-Tb) under mesophile conditions (Table 7).

Chemosynthesis in the water sample from the moire (sample 4622-M1-Tb) was less active, and its rate was comparable to that of CO_2 assimilation in water samples from black smokes (Table 7).

The fluid from a black smoke in field Q (sample 4668-M1-Tb) have a minimal rate of microbial chemosynthesis equal to no more than 100 ng C/l × day at incubation under thermophile conditions (Table 7). In diluted fluids from black smokers, the rates of chemosynthesis sometimes reach 3310 ng C/l × day (sample 4655-M2-Tb, Table 7), but these values characterize the microbial production of chemosynthesis in the solution discharge zone at the seafloor but not within the hydrothermal system with high temperatures of the solutions.

This also pertains to the intensity of other microbial processes. The processes of methane oxidation (to 577 nl C/l × day, Table 7) and biogenic sulfate reduction (2700 nl H_2S/l × day) are active in hot solutions and are mediated by thermophile microorganisms. Dozens of their species were collected from the solutions of a hydrothermal system in mid-oceanic ridges [25, 26].

Our experiments with solution samples from hydrothermal fields at 9°50′ N demonstrate a direct correlation of the rate of methane oxidation with the methane concentration in the solution, i.e., the dilution of the hot fluid by ambient seawater. In contrast to microbial chemosynthesis, the methanotrophic synthesis of C_{org} is more active in the least diluted solutions that have not lost their gas phase.

We are not aware of any published data on the rates of microbial processes in solutions from the hydrothermal system at 9°–10° N at EPR during its origin in 1991. Because of this, we are left with the only possibility of comparing our data with the results obtained on the rates of microbial processes in the hot solution of

Table 8. Rate of the dark bacterial assimilation of $^{14}CH_4$ in fluids from various hydrothermal fields

Active field	Brief characterization	$^{14}CO_2$ assimilation, ng C/l day	Reference
21° N, EPR	Hot solution, $t > 300$°C	240	[27]
14°45′ N, MAR (Logachev and Irina 2 fields)	Hot solution, $t > 300$°C	172	[12]
36° N, MAR (Rainbow field)	Hot solution, $t = 301$°C	10	[12]
9°50.7′ N, EPR, 2003	Hot solution, $t = 300$°C	100	This paper

mature hydrothermal systems in the Mid-Atlantic Ridge (MAR) (Table 8), for which similar values of the rates of $^{14}CO_2$ assimilation were obtained [12].

CONCLUSIONS

Analysis of geochemical, geophysical, and geological materials led us to conclude that the alternation of cycles of hydrothermal activity at 9°50′ N in EPR is controlled solely by the temporal variations in the volcanic activity, i.e., with the emptying of the crustal magmatic chamber during the paroxysmal period and the collapse of its roof leading to the origin of pathways for the ascent of hydrothermal solutions. The duration of a hydrothermal cycle is determined by the filling velocity of the magmatic chamber with basaltic melt. Tectonic cycles do not likely play significant role in the evolution of the hydrothermal activity in this high-spreading (~11–12 cm/year) EPR segment.

Over the twelve years of the evolution of the newly formed hydrothermal system, the diffuse outflow of hot fluids from fractures in the basaltic lavas gave way to focused seeps of hot solutions through channels in hydrothermal sulfide edifices.

The H_2S concentration in the hot solutions of field Q decreased by one order of magnitude from 1991 to 2003, whereas the contents of Cl, Fe, and Mn simultaneously increased and reached values characteristic of the solutions of the mature hydrothermal system at 21° N. This character of variations in the composition of the solution can be interpreted as a response to the disappearance of the surface boiling zone within the hydrothermal system. The Fe/H_2S ratio in the outpoured solution increased thereby a factor of 1.7 (from 0.36 to 0.61) and induced the disappearance of microbial mats from the hydrothermal fields in 2003.

The S isotopic composition of H_2S in the solution of field Q in 2003 differed from the isotopic composition of H_2S in the solution during the early evolution of the hydrothermal system in having a lower (by 2–3‰) concentration of the heavy ^{34}S isotope and approached the average values of $\delta^{34}S$–H_2S of the most currently known oceanic hydrothermal fields. There seems to be no correlation between the H_2S isotopic composition and its concentrations in solutions. The H_2S concentrations vary within broad limits (from 1 to 86 mM/kg), while the S isotopic composition of H_2S varies from 3 to 8‰ irrespective of the H_2S concentration, a fact testifying to the rapid evolution of the newly developing hydrothermal system during the first years of its lifetime (Fig. 3). We also cannot rule out that the variations in the concentration of H_2S and its isotopic composition are controlled by the existence of more than one source of S in the solutions, including a biogenic source.

The CH_4 concentration in the solutions in 2003 was close to the lower limit of CH_4 concentrations known to occur in solutions from 21° N (Table 3). Similar to the concentrations of other gases (H_2S, CO_2, and H_2), the CH_4 concentration in the fluids early in the evolution of the hydrothermal system was higher by one to two orders of magnitude.

Carbon in the CH_4 of the hot fluid from field Q in the sample collected in 2003 was depleted in the ^{13}C isotope ($\delta^{13}C = -22.0$‰, an average of three samples) compared to CH_4 in the solution from 21° N at EPR and had $\delta^{13}C$–CH_4 values close to those in the solution from the southern segment of EPR. The difference in the C isotopic composition of CH_4 from the young field Q and from more mature fields within EPR is as great as 5‰ and could also be caused by the occurrence of several CH_4 sources of the fluid in field Q.

We obtained the first data on the DOC concentrations in solutions from field Q. The hot solution (end member) contained 2 mg/l DOC, and the warm solution had approximately 6 mg/l DOC. The origin of the dissolved carbon-bearing compounds in the solutions is still uncertain.

The content of particulate matter in the hot fluid equals 632 mg/l, with 0.013–0.075% of the particulate material accounted for by C_{org}. The particulate material is dominated by sulfide minerals and iron hydroxides. The organic carbon of the particulate matter is depleted in the ^{13}C isotope by 16–26‰ relative to the carbon of the methane ($\delta^{13}C$–C_{org} of the particulate matter ranges from –36.7 to –48.0‰). The isotopically light composition of C_{org} of particulate matter from the hot solution can be explained by the isotopic–kinetic effect of both abiogenic synthesis [24] and biological processes. The involvement of biological material in the particulate matter also follows from the occurrence of microbial cells (cocci) and the results of experiments with labeled

substrates during incubation ($t = 70°C$), which made it possible to identify the active processes of methane anaerobic oxidation and sulfate reduction.

The C_{org} in the particulate matter of warm moire seeps is, conversely, enriched in the ^{13}C isotope, and its $\delta^{13}C$–C_{org} value approaches the average values of $\delta^{13}C$ for the biomass of free-living symbiotrophic microorganisms: the tissues of vestimentiferans and other species of the hydrothermal community with $\delta^{13}C$ from –11 to –35‰. In other words, the particulate matter from the moires is dominated by biogenic material.

The results of the complex chemical, microbiological, and isotopic research at the young evolving hydrothermal system at 9°50′7 N within EPR demonstrate that the chemical composition of the solutions evolved over the past twelve years and approached the composition of solutions in mature hydrothermal system at EPR. At the same time, newly obtained data on the cycle of carbon in the hydrothermal system highlighted new problems, first of all, the possibility of the abiogenic synthesis of carbon-bearing compounds and the role of the biogenic constituent in the overall carbon cycle in the hydrothermal system of fast-spreading ridges with buried hydrothermal biological communities.

ACKNOWLEDGMENTS

The authors thank G.A. Pavlova, V.V. Gordeev, L.L. Demina, Yu.M. Miller, and V.E. Erokhin for their chemical and isotopic analyses. This study was financially supported by the Russian Foundation for Basic Research, project nos. 03-05-64414, 03-05-64346, and 03-04-48945.

REFERENCES

1. W. C. Shanks III, "Stable Isotopes in Seafloor Hydrothermal Systems: Vent Fluids, Hydrothermal Deposits, Hydrothermal Alteration and Microbial Processes," in *Stable Isotope Geochemistry,* Ed. by J. W. Valley and D. R. Cole, Rev. Mineral. Geochem. **43**, 469–525 (2001).
2. K. L. von Damm, J. M. Grebmeier, and J. M. Edmond, "Preliminary Chemistry of Hydrothermal Vent Fluids from 9°–10° N East Pacific Rise," EOS Trans., AGU (1991).
3. K. L. von Damm, S. E. Oosting, R. Kozlowski, et al., "Evolution of East Pacific Rise Hydrothermal Vent Fluids Following a Volcanic Eruption," Nature **375**, 47–50 (1995).
4. K. L. von Damm, L. G. Buttermore, S. E. Oosting, et al., "Direct Observation of the Evolution of a Seafloor 'Black Smoker' from Vapor to Brine," Earth Planet. Sci. Lett. **149**, 101–111 (1997).
5. R. Haymon, D. Fornary, R. Lutz, et al., "Volcanic Eruption of the Mid-Ocean Ridge along the East Pacific Rise at 9°45′–52′ N: Direct Submersible Observations of Seafloor Phenomena Associated with an Eruption Event in April 1991," Earth Planet. Sci. Lett. **119**, 85–101 (1993).
6. K. L. von Damm, "Chemistry of Hydrothermal Vent Fluids from 9–10° N, East Pacific Rise: 'Time Zero,' the Immediate Posteruptive Period," J. Geophys. Res. **105** (5), 11 203–11 222 (2000).
7. T. M. Shank, D. J. Fornasi, K. L. von Damm, et al., "Temporal and Spatial Patterns of Biological Community Development at Nascent Deep-Sea Hydrothermal Vents (9°50′ N, East Pacific Rise)," Deep-Sea Res. **45**, Part II, 465–515 (1998).
8. R. Haymon, D. Fornary, R. Lutz, et al., "Dramatic Short-Term Changes Observed during March'92 Dives to April'91 Eruption Site on the East Pacific Ridge Crest, 9°54′ N," EOS Trans., AGU **73**, 524 (1992).
9. R. Haymon, D. Fornary, R. Lutz, et al., "1991 Eruptive Site on the East Pacific Rise at 94°5′–95°2′ N Is Evolving Rapidly: Results of Adventure'92 Dive Series," Ridge Events **3** (2), 1–11 (1992b).
10. R. Haymon, D. Fornary, M. H. Edwards, et al., "Hydrothermal Vent Distribution Along the East Pacific Rise Crest (9°09′–9°54′ N) and Its Relationship to Magmatic and Tectonic Processes on Fast-Spreading Mid-Ocean Ridges," Earth Planet. Sci. Lett. **104**, 513–534 (1991).
11. N. V. Pimenov, A. S. Savvichev, A. Yu. Lein, et al., "Microbial Processes of the Carbon Cycle as the Base of the Food Chain of the Hakon Mosby Mud Volcano Benthic Community," Geo-Mar. Lett. **19**, 89–96 (1991).
12. A. Yu. Lein and N. V. Pimenov, "Role of Bacterial Production at the Active Fields in a Total Balance of the Organic Carbon in the Ocean," in *Biology of Hydrothermal Systems* (KMK Ress, Moscow, 2002) [in Russian].
13. W. C. Shanks III, J. K. Bohlke, and R. R. Seal II, "Stable Isotopes in Mid-Ocean Ridge Hydrothermal Systems: Interactions between Fluids, Minerals, and Organisms," in *Seafloor Hydrothermal Systems: Physical, Chemical, Biological and Geological Interaction*, Ed. by S. E. Humphris et al., Geophys. Monograph Ser. **91**, 194–221 (AGU, Washington D.C., 1995).
14. M. D. Lilley, E. J. Olson, J. E. Lupton, and K. L. von Damm, "Volatiles in the 9° N Hydrothermal System: a Comparison of 1991 and 1992 Data," EOS. Trans., AGU (1992).
15. K. L. von Damm, "Seafloor Hydrothermal Activity Black Smoker Chemistry and Chimneys," Ann. Rev. Earth Planet. Sci. **18**, 173–204 (1990).
16. J. A. Welhan and H. Craig, "Methane, Hydrogen, and Helium in Hydrothermal Fluids at 21° N on the East Pacific Rise," in *Hydrothermal Processes at Seafloor Spreading Centers*, Ed. by P. A. Rona et al. (Plenum, New York, 1983), pp. 391–409.
17. E. Dounville, J. L. Charlou, E. H. Oelkers, et al., "The Rainbow Vent Fluids (36°14′ N, MAR): The Influence of Ultramafic Rocks and Phase Separation on Trace Metal Content in Mid-Atlantic Ridge Hydrothermal Fluids," Chem. Geol. **184**, 37–48 (2002).
18. D. V. Grichuk, *Thermodynamic Models of Submarine Hydrothermal Systems* (Nauchnyi Mir, Moscow, 2000) [in Russian].
19. J. L. Charlou, Y. Foquet, J. P. Donval, et al., "Mineral and Gas Geochemistry of Hydrothermal Fluids on an Ultrafast Spreading Ridge: East Pacific Rise, 17° to 19° S

(Naudur Cruise, 1993) Phase Separation Processes Controlled by Volcanic and Tectonic Activity," J. Geophys. Res. **101** (B7), 15899–15919.

20. M. D. Lilley, E. J. Olson, E. Molaughlin, and K. L. von Damm, "Methane, Hydrogen, and Carbon Dioxide in Vent Fluids from 9° N Hydrothermal System," EOS Trans., AGU **72**, (1991).
21. M. D. Lilley, D. A. Butterfield, J. E. Lupton, et al., "Anomalous CH_4 and NH^{4+} Concentrations at an Unsedimented Mid-Ocean Ridge Hydrothermal System," Nature **364** (6432), 45–47 (1993).
22. A. Yu. Lein, "Sulfur and Carbon Isotopes in Hydrothermal Fields of the Mid-Atlantic Ridge," Geokhimiya, No. 11, 1162–1173 (2001) [Geochem. Int. **39** (11), 1066 (2001)].
23. F. A. Alekseev, G. I. Voitov, V. S. Lebedev, and Z. N. Nesmelova, *Methane* (Nedra, Moscow, 1978) [in Russian].
24. J. Horita and M. Berndt, "Abiogenic Methane Formation and Isotopic Fractionation under Hydrothermal Conditions," Science **285** (5430), 1055–1057 (1999).
25. K. O. Stetter, "Hyperthermophilic Prokaryotes," FEMS Microbiol. Rev. **18**, 149–158 (1996).
26. E. A. Bonch-Osmolovskaya, "Thermophyle Microorganisms in Marine Hydrothermal Systems," in *Biology of Hydrothermal Systems* (KMK Press, Moscow, 2002) [in Russian].
27. D. M. Karl, "Bacterial Production at Deep-Sea Hydrothermal Vents and Cold Seeps: Evidence for Chemosynthetic Primary Production," in *Ecology of Microbial Communites*, Ed. by M. Fletcher, T. R. Gary, and J. G. Jones (Cambridge Univ., Cambridge, 1987), pp. 319–360.